Accepted Manuscript

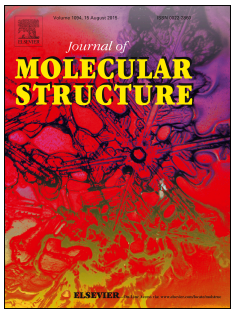

Synthesis, characterization and antimicrobial activity of some nickel, cadmium and mercury complexes of 5-methyl-3yl-N-(2′-methylthiophenyl)-methyleneimine, (MP_ZOATA) ligand

Susmita Mandal, Monojit Mondal, Jayanta Kumar Biswas, David B. Cordes, Alexandra M.Z. Slawin, Ray J. Butcher, Manan Saha, Nitis Chandra Saha

PII: S0022-2860(17)31193-6

DOI: 10.1016/j.molstruc.2017.09.015

Reference: MOLSTR 24264

To appear in: *Journal of Molecular Structure*

Received Date: 21 May 2017

Revised Date: 28 August 2017

Accepted Date: 8 September 2017

Please cite this article as: S. Mandal, M. Mondal, J.K. Biswas, D.B. Cordes, A.M.Z. Slawin, R.J. Butcher, M. Saha, N. Chandra Saha, Synthesis, characterization and antimicrobial activity of some nickel, cadmium and mercury complexes of 5-methyl-3yl-N-(2′-methylthiophenyl)-methyleneimine, (MP_ZOATA) ligand, *Journal of Molecular Structure* (2017), doi: 10.1016/j.molstruc.2017.09.015.

New Ni(II), Cd(II) and Hg(II) complexes of a pyrazole based Schiff base ligand, MP_zOATA, have been synthesized and physico-chemically & spectroscopically characterized. The structural conformations of the reported complex species have been established by single crystal X-ray studies. The emission properties and the antimicrobial activities of the metal ion materials have been reported.

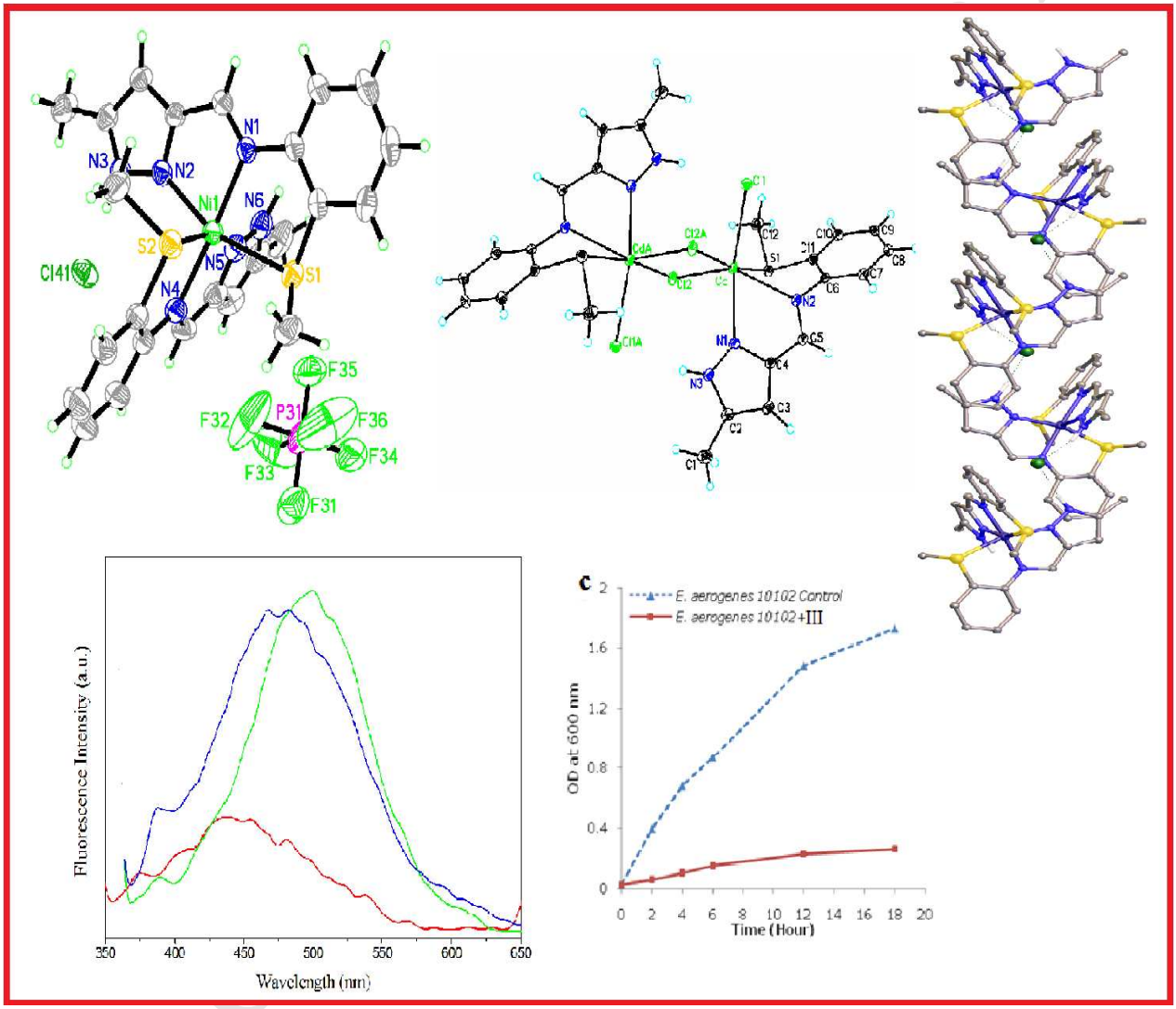

Synthesis, characterization and antimicrobial activity of some nickel, cadmium and mercury complexes of 5-methyl-3yl-N-(2´-methylthiophenyl)-methyleneimine, (MP_zOATA) ligand

Susmita Mandal[a], Monojit Mondal[b], Jayanta Kumar Biswas[b], David B. Cordes[c], Alexandra M. Z. Slawin[c], Ray J. Butcher[d], Manan Saha[a], Nitis Chandra Saha[a]*

[a] *Department of Chemistry, University of Kalyani, Nadia, West Bengal-741235, India*

[b]*Department of Ecological Studies and International Centre for Ecological Engineering, University of Kalyani Nadia, West Bengal-741235, India*

[c]*School of Chemistry, University of St Andrews, North Haugh, St Andrews, Fife, KY16 9ST U.K*

[d]*Department of Chemistry, Howard University, 525 College Street NW, Washington, DC 20059, USA*

Abstract

Herein, we report the syntheses and structures of Ni(II) complexes, $[Ni(MP_zOATA)_2]$ (Cl) (PF_6) (**I**), $[Ni(MP_zOATA)_2](ClO_4)_2.CH_3CN$ (**II**) & $[Ni(MP_zOATA)_2](BF_4)_2.H_2O$ (**III**); Cd(II) complex, $[Cd(MP_zOATA)Cl_2]_2$ (**IV**) and a Hg(II) complex, $[Hg(MP_zOATA)Cl_2]$ (**V**), of a pyrazole based 'NNS' donor ligand, 5-methylpyrazole-3yl-N-(2´-methylthiophenyl)methyleneimine, (MP_zOATA). The complexes are characterized by elemental analyses, electronic, IR, ^{1}H-NMR (only for **IV** & **V**) spectral parameters, conductivity and fluorescence measurements. X-ray crystallographic data of the complexes reveal that the Ni(II) complexes have NiN_4S_2 octahedral coordination, one of them is a mixed-anion complex having Cl^- and PF_6^- as counter anions; the Cd(II) complex is a chloro bridged binuclear complex with octahedral coordination environment around each metal centre, while the Hg(II) complex is a square pyramidal one. Among the reported complex species, the Ni(II) complexes are non-fluorescent, while the Cd(II) and Hg(II) complexes can be used as potential photoactive materials as indicated from their characteristic emission properties. The reported complexes are screened for their antimicrobial activities against some Gram positive and Gram negative microbial strains, and they are found to be

potential antimicrobial agents in broad spectrum against both Gram positive and Gram negative bacteria.

Keywords: Pyrazole, Schiff-base, Cd(II), Hg(II), X-ray Crystallography, Antibacterial potential,

*Corresponding author. Fax : +91-33-25828282; e-mail : nitis.saha@gmail.com

1. Introduction

Coordination chemistry of transition metal ions with various Schiff base ligands have been the area of interest in recent years because of wide range of geometry leading to structural diversity and application in various fields like biological, medicinal, analytical and as catalyst in organic reactions [1-16]. Schiff base ligands having Nitrogen-Sulfur as coordination sites towards metal ions, are important building blocks for metal-organic moieties. The chelating nitrogen and sulfur atoms can stabilize unusual oxidation states and uncommon coordination numbers in metal ion complexes [17]. During the last few years a significant attention has been given in using of heterocyclic compounds having nitrogen as donor site(s) for ligation with various transition metal ions; the π-electrons present on the hetero-atom(s) actively take part in the formation of stable metal-ligand (M-L) bonds during complex formation. Pyrazole (1:2 diazole), a five-membered nitrogen containing heterocycle, being isomeric with imidazole (1:3 diazole), an essential part of the well-known histidine residue of many proteins, has drawn substantial attention of chemists as a coordinating ligand for complexation since the reporting of $[Ag(pz)]_n$ in 1889 [18]; subsequently a large number of coordination complexes of pyrazole containing ligands with various biologically relevant transition metal ions like Fe(III), Co(III), Ni(II), Cu(II) etc. have been reported [19]. The application of coordination complexes with pyrazole containing ligands as biological models is well-documented [20]. Among the transition metal ion complexes, investigation of nickel compounds is of great interest in chemistry for their renowned bioactivity and catalytic activity in many organic reactions [21-24]. On the other hand d^{10} metal ions are well recognized for their catalytic activity, emissive property and application as opto-electronic materials, and uses in environmental chemistry [25-28]. The coordination chemistry of cadmium and mercury is the point of interest, because of the facts that the ions are

capable of affording a number of coordination numbers and geometries owing to their d^{10} configuration; their toxic environmental effects, mobilization and immobilization in the environment, in living organisms, and in certain chemical processes like ligand exchange chromatography depend remarkably on their complexation with ligands having nitrogen as donor site(s) [29]. With this background and in continuation of our previous work [30], this communication is intended to report the syntheses and characterizations of Ni(II), Cd(II) and Hg(II) complexes of a 'NNS' tridentate ligand, 5-methylpyrazole-3yl-N-(2´-methylthiophenyl)-methyleneimine (MP_zOATA) (Figure 1) together with the fluorescence emission of the Cd(II) and Hg(II) complexes at room temperature. The antimicrobial properties of the synthesized complexes are analyzed in vitro against some Gram positive and Gram negative bacterial strains.

2. Experimental

2.1. Materials and physical measurements

All the solvents and reagents were of AR/GR grade and obtained from commercial sources and used without further purification. Spectral and conductance measurements were performed using spectrograde solvents. Elemental analyses (C, H and N) were done with a Perkin-Elmer 2400 CHNS/O analyzer. The molar conductance values of the complexes in methanol (CAS NO. 67-56-1) were measured with a Systronics 306 digital conductivity meter. The electronic spectra and the diffuse reflectance spectra were recorded on a Shimadzu UV-2401PC spectrophotometer. IR spectra (4000-450 cm^{-1}) were recorded on a Perkin Elmer L120-000A FT-IR spectrophotometer with KBr pellets (CAS No. 7758-02-3). ^1H NMR spectra for the complexes were recorded in d_6-DMSO (CAS No. 2206-27-1) with a Bruker AC 400 NMR spectrometer. The fluorescence

spectra of the complexes in methanol were recorded using a Perkin-Elmer LS 55 Fluorescence Spectrometer.

2.2. Syntheses

2.2.1. Synthesis of ligand, MP_zOATA

The title ligand, MP_zOATA, had been synthesized and thoroughly characterized by various physico-chemical & spectral parameters, as reported in an earlier communication [30a].

*2.2.2. Syntheses of complexes, $[Ni(MP_zOATA)_2]$ (Cl) (PF_6) (**I**), $[Ni(MP_zOATA)_2](ClO_4)_2$. CH_3CN (**II**), $[Ni(MP_zOATA)_2]$ $(BF_4)_2.H_2O$ (**III**), $[Cd(MP_zOATA)Cl_2]_2$ (**IV**) and $[Hg(MP_zOATA)Cl_2]$ (**V**)*

The complex **I** was synthesized by refluxing together methanol solutions of the primary ligand, MP_zOATA (0.00105 mol) and $NiCl_2.6H_2O$ (CAS No. 7791-20-0) (0.000525 mol) on water bath for ~1 hour; then 0.00105 mole solid KPF_6 (CAS No. 17084-13-8) was added slowly with stirring for an hour. On slow evaporation of the resulting solution, dark brown shiny crystalline solid separated out, was filtered off, washed with cold methanol and finally dried over anhydrous $CaCl_2$ (yield~75%). Diffractable quality single crystals of $[Ni(MP_zOATA)_2]$ (Cl) (PF_6) were obtained on slow evaporation of the methanol solution of the complex. Similarly, complexes **II** and **III** were synthesized by refluxing mixture of methanol solutions of the ligand (0.00105 mol) and $Ni(ClO_4)_2.6H_2O$ (CAS No. 13520-61-1) / $Ni(BF_4)_2.6H_2O$ (CAS No. 13877-16-2) (0.000525 mol), on water bath for ~1 hour. On slow evaporation of the resulting reaction mixtures, each of the desired Ni(II) complex separated out as brown crystalline solid, was filtered off, washed with cold methanol and was dried over anhydrous $CaCl_2$ (yield ~75-80%). X-ray quality single crystals of **II** and **III** were obtained on slow crystallization of the acetonitrile (CAS No. 75-05-8) and methanol solution of the respective complexes. The complexes **IV** and **V** had been

synthesized by refluxing together equimolar (0.00105 mol) mixture of the primary ligand and $CdCl_2.2H_2O$ (CAS No. 72589-96-9) / $HgCl_2$ (CAS No. 7487-94-7) in ethanol, on water bath for ~1 hour. The desired complex, in each case, separated out as colorless crystalline solids upon slow evaporation of the resulting reaction mixture, was filtered off, washed with cold ethanol and was allowed to dry over anhydrous $CaCl_2$ (yield ~70-80%). Single crystals of $[Cd(MP_zOATA)Cl_2]_2$ and $[Hg(MP_zOATA)Cl_2]$ obtained on slow evaporation of the reaction mixtures of the complex species were found suitable for X-ray diffraction.

Anal. Calcd.(%) for $C_{24}H_{26}ClF_6N_6PS_2Ni$ **(I)**: C, 41.0; H, 3.7; N, 11.9; Ni, 8.4. Found (%): C, 40.8; H, 3.5; N, 12.1; Ni, 8.3. Anal. Calcd. (%) for $C_{26}H_{29}Cl_2N_7O_8S_2Ni$ (**II**): C, 40.9; H, 3.8; N, 12.9; Ni, 7.7. Found (%): C, 40.6; H, 3.5; N, 13.0; Ni, 7.4. Anal. Calcd. (%) for $C_{24}H_{28}B_2N_6F_8OS_2Ni$ (**III**): C, 40.4; H, 3.9; N, 11.8; Ni, 8.2. Found (%): C, 40.3; H, 3.7; N, 12.0; Ni, 8.1. Anal. Calcd. (%) for $C_{24}H_{26}Cd_2Cl_4N_6S_2$ (**IV**): C, 34.7; H, 3.2; N, 10.1; Cd, 27.1. Found (%): C, 34.3; H, 3.0; N, 10.3; Cd, 26.8. Anal. Calcd. (%) for $C_{12}H_{13}N_3Cl_2SHg$ (**V**): C, 28.6; H, 2.6; N, 8.4; Hg, 4.0. Found(%): C, 28.3; H, 2.6; N, 8.5; Hg, 3.7.

2.3. Structure determination

X-ray diffraction data of the complex species were collected either at 173 K (**I**) using a Rigaku FR-X Ultrahigh Brilliance Microfocus RA generator/confocal optics and XtaLAB P200 system (Mo Kα radiation, λ = 0.71073 Å), at 295 K (**II**) by using an Agilent Xcalibur Gemini diffractometer with graphite monochromator and Ruby CCD system (Cu Kα radiation, λ = 1.54178 Å), at 93 K (**III**) by using a Rigaku MM007 High Brilliance RA generator/confocal optics and Mercury 70 CCD system (Mo Kα radiation, λ = 0.71073 Å), or at 123 K (**IV** and **V**) by using an Agilent Xcalibur Gemini diffractometer with graphite monochromator and Ruby

CCD system (Mo Kα radiation, λ = 0.71073 Å). Intensity data were collected using ω steps (**I**, **II**, **IV** and **V**) or both ω and φ steps (**III**) accumulating area detector images spanning at least a hemisphere of reciprocal space, and were corrected for Lorentz polarization and absorption effects. Multiscan absorption corrections were applied using Crystal Clear [31] (**I** and **III**) or the SCALE3 ABSPACK scaling algorithm implemented in CrysAlisPro v1.171.35.11 [32] (**V**), and analytical absorption corrections were applied using a multifaceted crystal model [33] implemented in CrysAlisPro v1.171.35.11 [32] (**II** and **IV**). The structures were solved by direct (SIR2004 [34], SHELXS-97 [35]) or Patterson methods (DIRDIF99 PATTY [36]) and refined using full-matrix least squares (SHELXL-2013 [37] and SHELXL-97 [35]). All aliphatic and aromatic hydrogen atoms were assigned riding isotropic displacement parameters and constrained to idealized geometries. Hydrogen atoms bound to N or O in **I** or **III** were located from the difference Fourier map and refined subject to a distance restraint, while those in the other structures were assigned riding isotropic displacement parameters and constrained to idealized geometries. The crystallographic data are summarized in Table 1.

2.4. Antimicrobial Activity

In vitro antimicrobial analyses were performed to evaluate the antimicrobial potential of those synthesized compounds under study against six selected bacterial strains namely *Salmonella enterica ser. typhi* SRC, *Proteus vulgaris* OX19, *Bacillus subtilis* 6633, *Enterobacter aerogenes* 10102, *Staphylococcus aureus* and *Escherichia coli* K12. Those microbial strains comprising of two Gram positive and four Gram negative ones, were obtained from Microbial Type Culture Collection and Gene Bank (MTCC), Institute of Microbial Technology, Chandigarh and Department of Microbiology, University of Kalyani. Amoxicillin (CAS No. 61336-70-7), a

clinically recommended antibacterial agent was used as the reference antimicrobial agent [30a]. The compounds were dissolved in dimethyl sulfoxide (DMSO) (CAS No. 67-68-5) and final concentration of DMSO was maintained constant (up to 1%). Nutrient Broth /Agar (Modified) was used for *in vitro* antimicrobial analysis and minimum inhibitory concentrations (MIC) of these compounds were determined as per NCCLS protocol [38]. Bacterial susceptibility of these compounds was assessed using agar well diffusion method [39]. Subjected to those compounds the microbial growth kinetics was evaluated with two bacterial strains (*Bacillus subtilis* 6633 and *Enterobacter aerogenes* 10102).

Bacterial membrane damage assay was also performed to further verify the efficacy of the complexes on bacterial cell membrane integrity. Membrane damage was determined by quantifying the quantum of nucleic acids released from the cell interior [40, 41]. This assay was performed on a gram positive (*Bacillus subtilis* 6633) and a gram negative (*Proteus vulgaris* OX19) bacterial strain as representative from two distinct groups under study. Overnight culture of both the bacterial strains was centrifuged at 7000 rpm for 5 min. The cell pellet was washed thrice with phosphate buffer saline (PBS, pH 7.4) and resuspended in the specific liquid culture media. The optical density of the bacterial suspension was set 0.8 at 420 nm and distributed into different conical flasks. The concentration of the complexes was set at the specific MIC of the individual complexes determined beforehand against the bacterial strains. A control set was prepared without addition of the complexes. In every one hour two mL of sample was collected and filtered with 0.2 µm syringe filter and the filtrate was measured at 260 nm in a UV-Vis spectrophotometer to estimate the amount of nucleic acids released in the mean time.

3. Results and discussion

The title ligand, MP_ZOATA, was characterized by elemental analyses (C, H and N), IR, ^{1}H-NMR and mass spectrum studies and the results had been reported earlier [30a].

3.1. Characterization of the complexes

The reported complexes gave satisfactory C, H, N and metal analyses and conformed to the composition as $[Ni(MP_zOATA)_2](PF_6,Cl)$ **I**, $[Ni(MP_zOATA)_2](ClO_4)_2.CH_3CN$ **II**, $[Ni(MP_zOATA)_2](BF_4)_2.H_2O$ **III**, $[Cd(MP_zOATA)Cl_2]_2$ **IV** and $[Hg(MP_zOATA)Cl_2]$ **V**. The molar conductance values in MeOH (30°C) classified **I**, **II** and **III** as 1:2 electrolytes (λ_M = 230, 280 and 229 $ohm^{-1}cm^2mol^{-1}$ for **I**, **II** and **III,** respectively); **IV** and **V** as non-electrolytes (λ_M= 45 and 58 $ohm^{-1}cm^2mol^{-1}$, respectively) [42].

The characteristic IR bands (4000-450 cm^{-1}) provided meaningful information regarding the binding sites of the primary ligand molecules with the central metal ions. IR bands appeared in the region (1595-1608 cm^{-1}) in the complex species are consistent with the coordination of the azomethine nitrogen (CH=N) to the central metal ion, whereas bands obtained at 469-473 cm^{-1} are then assignable to $\nu_{(M\text{-}N\ azomethine)}$. IR bands found at 1568-1578 cm^{-1} are indicative of participation of the tertiary ring nitrogen atom (^{2}N) as potential binding site [30, 43].

The diffuse reflectance spectral data of the reported Ni(II) complex are similar in nature and exhibited three bands in the regions 788-879 nm [$^3A_{2g}$ (F)→$^3T_{2g}$ (F)(ν_1)], 635-659 nm [$^3A_{2g}$ (F)→$^3T_{1g}$ (F)(ν_2)] and 331-405 nm [$^3A_{2g}$ (F)→$^3T_{1g}$ (P)(ν_3)], which correspond to an overall octahedral symmetry. The electronic spectra of the Ni(II) complexes in methanol are found to exhibit two bands in the regions 810-818 nm (ν_1) and 524-532 nm (ν_2), which are nearly similar to those found in the solid state, thereby suggesting no gross electronic or geometric change of the complex species has taken place on dissolution in the said solvent. The ν_3 band generally

appears due to $^3A_{2g}$ (F) → $^3T_{1g}$ (P) transition in the UV region was absent, this may be obscured by intense internal π→π* transition of the ligand or intense CT absorption bands [19b, 44].

The electronic spectra of complexes **IV** and **V** in methanol, have been found to exhibit two bands in the regions 206-208 nm and 251-254 nm, are attributed to the π-π* transition and one broad band appeared in the region 336-345 nm, may be assigned to the intra-ligand n-π* transition of the azomethine group [30b].

^{1}H NMR spectral data of the complexes **IV** and **V** when compared to those of the free ligand molecule, offered supportive information regarding the bonding characteristics of the primary ligand system in forming complexes with the concerned metal ions through the pyrazolyl ring nitrogen ^{2}N(tertiary), azomethine nitrogen and thioether sulfur atom. It has been observed that peaks for the azomethine proton and C_4-H (pyrazole ring) have been shifted to downfield regions in comparison to the free ligand (6.20 and 8.37 ppm for C_4-H of pyrazole ring and azomethine proton, respectively); and singlets at δ 8.35-8.59 and 9.80-9.26 ppm, respectively, have been found. Whereas the C_5-CH_3 protons of pyrazole moiety suffered up field shifts at δ, 1.02-1.79 ppm (δ=2.29 ppm for free ligand), and signal for S-CH_3 protons have been found to shift to downfield (at δ= 2.53-3.15 ppm) in comparison to the free ligand (δ=2.33 for free ligand). The N-H(pyrazole) proton appeared in the downfield region δ=13.51-13.16 ppm (δ=12.99 for free ligand).

3.2. Structural description

The complex **I** crystallizes in monoclinic *C2/c* space group, whereas complexes **II** and **III** crystallize in monoclinic $P2_1/n$ space group and complexes **IV** and **V** crystallize in triclinic P-1 space group. The Molecular view with atom numbering scheme for **I**, **II**, **III**, **IV** and **V** are

shown in Figs 2, 3, 4, 5 and 6 respectively and some selected bond lengths and angles are given in Table-2. Ni(II) has a distorted octahedral coordination in the complex species **I**, **II** and **III,** having NiN_4S_2 chromospheres. A pair of MP_zOATA ligands co-ordinates to the Ni(II) ion through the thioether sulfur, the tertiary nitrogen of the pyrazole ring and the azomethine nitrogen atoms. The two tridentate ligands bind Ni(II) centre one equatorially and the other trans-axially.

The crystallographic asymmetric unit in complex **I** consists of a $[Ni(MP_zOATA)_2]^{2+}$ cation and two different counter anions, Cl^- and PF_6^-, whereas, in complex **II** it comprises of $[Ni(MP_zOATA)_2]^{2+}$ cation, two ClO_4^- anions and one molecule of acetonitrile as the solvent of crystallisation, H-bonded with the pyrazolyl secondary nitrogen. The crystallographic asymmetric unit in complex **III** is similar to that in **I** and **II**, except that **III** contains two BF_4^- as counter ions along with one molecule of water of crystallization. In **I**, two molecules of the (NNS) tridentate ligand, MP_zOATA, coordinate to the Ni(II) ion to form four five-membered chelate rings, [Ni1-S1-C1-C2-N1, Ni1-S2-C13-C14-N4, Ni1-N1-C8-C9-N2A and Ni-N4-C20-C21-N5]. The two azomethine nitrogen atoms are *trans* to each other, while the pyrazolyl ring nitrogen atoms and the sulphur atoms are in the *cis* positions. The coordination patterns of the in **II** and **III** are identical, except that we do not refer to the individual members of the pair of ligands as they are related by symmetry. The tridentate ligands in all the Ni(II) complexes are more or less planar, and the pair of coordinating ligands is nearly orthogonal to each other with the (acute) dihedral angles (between the pair of coordinating ligands) of 84.12º, 89.01º and 86.63º for **I**, **II** and **III**, respectively. The geometry about the Ni(II) ions in all the complexes compare well with those reported for other similar structures [45]. In **I**, the $[Ni(MP_zOATA)_2]^{2+}$ cations are connected by the Cl^- anions through N-H...Cl H-bonding interactions and 1D infinite

chain has been generated running along the *b* axis. The pyrazolyl secondary nitrogen is acting as H-bond donor and involved in hydrogen bonding with the Cl atom (potential hydrogen-bond acceptor). The N–H, H...Cl and N...Cl distances are 0.95(18)-0.992(18), 2.12(2)-2.10(2) and 3.044(3)-3.040(3) Å respectively, and the N–H...Cl angles are 163 and 159º (Fig. S1).

In **II,** the ClO_4^- anion and one acetonitrile solvent molecule are bonded to cation $[Ni(MP_zOATA)_2]^{2+}$ by N(3A)-H(3AB)...O(21) and N(3B)-H(3BB)...N(1S) hydrogen bonding. One of the two ClO_4^- anions forms H-bonding with the cation through pyrazolyl nitrogen atom, whereas the other one is connected to the cation through the solvent molecule. The pyrazolyl secondary nitrogen is acting as hydrogen-bond donors with oxygen atom of perchlorate anion and nitrogen atom of solvent molecule as potential hydrogen-bond acceptors. The N-H, H...O and H…N(S), N...O and N…N(S) distances are 0.86, 1.98 and1.86, 2.829(4) and 2.719(5) Å respectively. The < (DHA) angles are170.5 and 172.9° (Fig. S2).

In **III,** the fluoroborate and water molecule are bonded to the cation by N33-H33N…F6[2] and N13-H13…O40[1]hydrogen bondings. The N-H, H...F and H…O, N...F and N…O distances are 0.98, 1.80(3) and 1.82(3), 2.770(4) and 2.753(5) Å, respectively. The < (DHA) angle are 171(3) and 159(4)° respectively. In complex **III** intra-molecular hydrogen bonding was found between the pyrazole ring nitrogens as N13-H13…N12 and N33- H33N…N32 (Fig. S3).

The unit cell of complex **IV** contains dinuclear neutral unit $[Cd(MP_zOATA)Cl_2]_2$ in which two mononuclear $Cd(MP_zOATA)Cl$ units are bridged by two chloride ions. The complex species is a centrosymmetric dimer, the inversion centre is located at the midpoint between the two cadmium atoms. Each metal centre is six coordinated by one molecule of MP_zOATA ligand, bonded to the Cd(II) ion in a tridentate mode through the pyrazolyl (tertiary) ring nitrogen atom, [N1], azomethine nitrogen atom, [N2] and thioether sulfur atom [S1], forming two five-membered

chelate rings, [Cd-S(1)-C(11)-C(6)-N(2) and [Cd-N(2)-C(5)-C(4)-N(1)]; the other three coordination sites are occupied by two bridging and one non bridging chloride ions. Thus each cadmium (II) ion centre has a distorted octahedral coordination with CdN_3SCl_3 chromophore. The two non-bridging chlorine atom on each metal centre are trans to each other. The Cd···Cd distance is 3.689(3) Å, longer than the sum of van der Waals radii of cadmium (3.2 Å), [30b], indicating no effective intermetallic interaction. The two bite angles, N(2)–Cd–N(1) and N(2)–Cd–S(1) of the five-membered chelate rings formed with the donor atoms N(2), N(1) and S(1) are 69.11(8) and 63.68(5) Å, respectively, indicating the largest distortion from the ideal octahedral geometry. Intra-molecular N-H...Cl contacts are observed between the secondary pyrazolyl nitrogen atoms (as H-atom donor) and the non-bridging chlorine atoms (as potential H-bond acceptor) (Fig. S4). The N-H, H...Cl and N…Cl distances are found to be 0.88, 2.42 and 3.286(2) Å respectively and the < (DHA) angle is 166.5°.

The asymmetric unit of complex **V** comprises of a Hg(II) ion, one unit of the neutral MP_zOATA ligand and two coordinated chlorine atoms. The Hg(II) centre, having a HgN_2SCl_2 chromophore with a distorted square pyramidal geometry. The basal plane of the pyramid is formed by the pyrazolyl (tertiary) ring nitrogen atom, [N1], the azomethine nitrogen atom, [N2], one thioether sulfur atom [S2] of the coordinating ligand and one coordinated chlorine atom [Cl2]; the other coordinated chlorine atom [Cl1] occupies the apical position. The Hg–N bond distances vary in the range 2.413(4)–2.444(3) Å, while the Hg–S bond distance is 2.7505(10) Å. The basal mercury (II)–chlorine [Hg1–Cl2] distance is 2.4853(9) Å, while the axial mercury (II)–chlorine [Hg1–Cl1] distance is 2.4145(9) Å. In this complex, the geometric parameter τ is 0.21, indicating displacement from an ideal square-pyramidal geometry [19e, 46]. In the structure, each monomeric metal–organic unit is connected by N–H...Cl hydrogen bonding interactions, formed

between the secondary nitrogen atom of pyrazole and axial chlorine atom, leading to the formation of a dimer. These dimmers are further assembled by C-H...Cl hydrogen bonding interactions between azomethine carbon and another axial chlorine atom and form 1D supramolecular chains. The N–H, H...Cl and N...Cl distances and the N–H...A angle are found to be 0.88, 2.32 and 3.133(3) Å and 153.2°, respectively, and in C-H...Cl contacts, the C-H, H...Cl and C...Cl distances and the C-H...Cl angle are 0.95, 2.776 and 3.528(4) Å and 136.8°, respectively (Fig. S5)

3.3. Fluorescence spectral study

Fluorescence spectra of the complexes were recorded in methanol ($2x10^{-5}$M) at room temperature. The complexes **I**, **II** and **III** are non-fluorescent, but complexes **IV** and **V** have shown characteristic fluorescence emissions. The fluorescence spectra of the complexes are shown in Fig.7. Intense emission bands for complex **IV** are observed at 503 nm when excited at 254nm, but abrupt change of fluorescence emission intensity and wavelength at 432 nm was observed on changing the excitation wavelength at 336 nm. However, no appreciable emission was observed on changing the wavelength for complex **V** for which emission maxima was observed at 478 nm (λ_{ex} = 251 nm). As Cd^{2+} and Hg^{2+} ions are difficult to be oxidized or reduced due to their stable d^{10} configuration, the emissions of their compounds cannot be attributed to either a metal-to-ligand charge transfer (MLCT) or a ligand to metal charge transfer (LMCT), and the primary ligand is also non-fluorescent. Therefore, the observed fluorescence intensity of the complex species may be attributed to increase in the conformational rigidity of the ligands due to chelate formation, which causes decrease in non-radiative decay of intra-ligand excited

states through vibrational motion [30b, 47-50]. The findings indicate that the complex species may be regarded as brilliant aspirants for photoactive material.

3.4. Antimicrobial activity

All the synthesized compounds under study showed active antimicrobial properties against six selected bacterial strains, but ligand did not exhibit any antimicrobial activity [16]. This may be due to ligand's limited solubility in DMSO. The MIC values and inhibition zone diameters for these compounds are presented in Table 3 and 4. Complex **I**, **II** and **III** showed antimicrobial activity beyond the concentrations of 1225, 1000 and 750µg/mL, respectively. These three compounds were found to show antimicrobial property against a wide range of bacterial strains. Complex **IV** showed its MIC value in the range of 25-175 µg/mL. The bacterial strains *Staphylococcus aureus* and *Proteus vulgaris* OX19 were most sensitive against **IV** with MIC concentration of 25 and 35 µg/mL, respectively. With overall MIC values ranging from 5 to 55 µg/mL, complex **V** exhibited an encouraging efficacy on *Proteus vulgaris* OX19 and *Staphylococcus aureus* with MIC concentrations of 5 and 20 µg/mL, respectively. All the five reported compounds showed broad spectrum antibacterial activity, being effective against both Gram positive and Gram negative microorganisms. The *in vitro* growth curves of two different bacterial species (*Enterobacter aerogenes* 10102 and *Bacillus subtilis* 6633) tested against the compounds as shown in Fig. 8 and Fig. 9, implied that the compounds tested have promising potential in inhibiting bacterial growth and hence can be effective as bacteriostatic agents.

The result showed that membrane damage was inflicted by all the complexes, in general and was very significantly intensified ($P< 0.05$) by complex **IV** and **V**, in particular. With lapse of time the adverse effect increased (Fig. 10). Among the five complexes complex **IV** and **V**

showed encouraging efficiency in membrane damage against both gram positive (*Bacillus subtilis* 6633) and gram negative (*Proteus vulgaris* OX19) bacterial strain showing its wide window of antibacterial efficacy. This observation draws support from antimicrobial results involving some other complexes [51] Bacterial cell membrane acts as physiological barrier against the biocidal agents [41]. Hence such membrane damage assay reinforced our aforesaid antibacterial activity of the studied complexes by presenting their mechanism of antibacterial action through damage in membrane integrity.

5. Conclusion

Herein we intend to report the syntheses, spectral and structural characterization of some Ni(II), Cd(II) and Hg(II) complexes of a pyrazole containing Schiff base ligand, 5-methylpyrazole-3yl-N-(2´-methylthiophenyl) methyleneimine, MP_zOATA. Single crystal x-ray studies have authenticated all the three Ni(II) complexes as monomeric octahedral species. In Cd(II) complex, two metal centers are bridged by two chloride ions and each one have octahedral coordination. Whereas Hg(II) complex is monomeric square pyramidal one. Furthermore, the intense fluorescence property of the Cd(II) and Hg(II) complexes at room temperature, suggests that they have potential applications as photoactive materials. It has also been shown that the synthesized complexes have immense potential to act as broad-spectrum antimicrobial agents against both Gram positive and Gram negative bacteria through disruption of cell membrane integrity.

Acknowledgement

One of us (S.M.) is thankful to the U.G.C., Govt. of India for providing financial support in the form of fellowship (*vide* UGC Award No.: File No. 17-81/2008 (SA-I) dated: 04.1.2011). The financial support received from the University of Kalyani in the form of Personal Research Grant is thankfully acknowledged.

Appendix A. Supplementary data

Crystallographic data for the structures reported here have been deposited with the Cambridge Crystallographic Data Centre, CCDC nos. 1004238, 903321, 965608, 1048324, 1048330. Copies of this information may be obtained free of charge from the Director, CCDC, Data Centre, 12 Union Road, Cambridge, CB2 1EZ, UK (fax: +44-1223-336-033; e-mail: deposit@ccdc.cam.ac.uk or http://www.ccdc.cam.ac.uk). Figs. S1-S5 are available as supplementary material.

References

[1] S. Arulmurugan, H.P. Kavitha, B.R. Venkatraman, Rasayan J. Chem. 3 (2010) 385-410.

[2] L.H. Abdel-Rahmana, R.M. El-Khatiba, L.A.E. Nassr, A.M. Abu-Dief, F. El-DinLashin, Spectrochim. Acta, Part A 111 (2013) 266.

[3] Z. Wu, D. Xu, Z. Feng, Polyhedron 20 (2001) 281.

[4] D.J. Darensbourg, O. Karroonnirun, Inorg. Chem. 49 (2010) 2360.

[5] (a) A.-N. M.A. Alaghaz, M.E. Zayed, S.A. Alharbi, R.A.A. Ammar, A. Elhenawy, Journal of Molecular Structure 1084 (2015) 352; (b) R.A. Ammar, A.-N.M.A. Alaghaz, M.E. Zayed, L.A. AL-Bedair, Journal of Molecular Structure (2017), doi: 10.1016/j.molstruc.2017.03.080 (and references therein)

[6] P.G. Cozzi, Chem. Soc. Rev. 33 (2004) 410.

[7] (a) R. Ziessel, Coord. Chem. Rev. 216–217 (2001) 195; (b) K.C. Gupta, A.K. Sutar, Coord. Chem. Rev. 252 (2008) 1420; (c) A. Garoufis, S.K. Hadjikakou, N. Hadjiliadis, Coord. Chem. Rev. 253 (2009) 1384

[8] J.P. Costes, S. Shova, W. Wernsdorfer, J. Chem. Soc., Dalton Trans. (2008) 1843.

[9] X.G. Ran, L.Y. Wang, Y.C. Lin, J. Hao, D.R. Cao, Appl. Organometal. Chem. 24 (2010) 741.

[10] M. Orio, O. Jarjayes, H. Kanso, C. Philouze, F. Neese, F. Thomas, Angew. Chem., Int. Ed. 49 (2010) 4989.

[11] S.A. Sadeek, M.S. Refat, S.M. Teleb, Bull. Chem. Soc. Ethiop. 18 (2004) 149.

[12] (a) M.S. Karthikeyan, D.J. Prasad, B. Poojary, K.S. Bhat, Bioorg. Med. Chem. 14 (2006) 7482.

[12] (b) K. Singh, M.S. Barwa, P. Tyagi, Eur. J. Med. Chem. 41 (2006) 147.

[13] (a) S.K. Sridhar, M. Saravanan, A. Ramesh, Eur. J. Med. Chem. 36 (2001) 615 ;
(b) P. Pannerselvam, R.R. Nair, G. Vijayalakshmi, E.H. Subramanian, S.K. Sridhar, Eur. J. Med. Chem. 40 (2005) 225.

[14] R. Mladenova, M. Ignatova, N. Manolova, T.S. Petrova, I. Rashkov, Eur. Polym. J. 38 (2002) 989.

[15] O.M. Walsh, M.J. Meegan, R.M. Prendergast, T.A. Nakib, Eur. J. Med. Chem. 31 (1996) 989.

[16] A. Chakraborty, P. Kumar, K. Ghosh, P. Roy, Eur. J. Pharmacol. 647 (2010) 1.

[17] M. Hossain, S.K. Chattopadhyay, S. Ghosh, Polyhedron 16 (1997) 1793 (and references therein).

[18] E .Büchner, Ber. Dtsch. Chem. Ges. 22 (1889) 842.

[19] (a) N.C. Saha, R.J. Butcher, S. Chaudhuri, N. Saha, Polyhedron 21 (2002) 779 (and references therein); (b) N.C. Saha, R.J. Butcher, S. Chaudhuri, N. Saha, Polyhedron 24 (2005) 1015 (and references therein); (c) D.K. Sau, R.J. Butcher, S. Chaudhuri, N. Saha, Molecular and Cellular Biochemistry 253 (2003) 21 (and references therein); (d) N.C. Saha, C. Biswas, A. Ghorai, U. Ghosh, S.K. Seth, T. Kar, Polyhedron 34 (2012) 1(and references therein); (e) S. Mandal, R. Sadhukhan, U. Ghosh, S. Mandal, M. Saha, R.J. Butcher, N.C. Saha, J. Coord. Chem. 69 (2016) 1618 (and references therein)

[20] A. Chauhan, P.K. Sharma, N. Kaushik, Int. J. ChemTech Res. 3 (2011) 11

[21] F.H. Haghighi, H. Hadadzadeh, F. Darabi, Z. Jannesari, M. Ebrahimi, T. Khayamian, M. Salimi, H. A. Rudbari, Polyhedron 65 (2013) 16.

[22] M. Jesmine, M.M. Ali, A.K. Biswas, M.R. Habib, J.A. Khanam, Med. J. Islam W. Acad. Sci. 16 (2008) 135.

[23] Y. Yang, P. Yang, C. Zhang, G. Li, X. J. Yang, B. Wu, C. Janiak, J. Mol. Catal. A Chem. 296 (2008) 9.

[24] S.M. Nelana, J. Darkwa, I.A. Guzei, S.F. Mapoli, J. Organomet. Chem. 689 (2004) 1835.

[25] K.A. Siddiqui, G.K. Mehrotra, S.S. Narvi, R.J. Butcher, Inorg. Chem. Comm. 14 (2011) 814 (and references therein).

[26] M. Li, L. Liu, L. Zhang, X. Lv, J. Ding, H. Hou, Y. Fan, Cryst. Eng. Comm. 16 (2014) 6408.

[27] P. Orioli, B. Bruni, M.D. Vaira, L. Messori, F. Piccioli, Inorg. Chem. 41 (2002) 4312.

[28] O.A. El-Gammal, G.M.A. El-Reash, M.M. El-Gamil, Spectrochim. Acta. Mol. Biomol. Spectros. 123 (2014) 59.

[29] J.N. Le Pag, W. Lindner, G. Davies, D.E. Seitz, B.L. Karger, Anal. Chem. 51 (1979) 433.

[30] (a) N.C. Saha, S. Mandal, M. Das, N. Khatun, D. Mitra, A. Samanta, A.M.Z. Slawin, R.J. Butcher, R. Saha, Polyhedron 68 (2014) 122; (b) S. Mandal, R. Saha, M. Saha, R. Pradhan, R.J. Butcher, N.C. Saha, Journal of Molecular Structure 1110 (2016) 11.

[31] *CrystalClear-SM Exper*t v2.0 and v2.1. Rigaku Americas, the Woodlands, Texas, USA, and Rigaku Corporation, Tokyo, Japan, (2010-2014).

[32] CrysAlisPro, Agilent Technologies, Version 1.171.35.11(release 16-05-2011).

[33] R. C. Clark, J. S. Reid, Acta. Crystallogr., Sect. A. 51(1995) 887.

[34] M. C. Burla, R. Caliandro, M. Camalli, B. Carrozzini, G.L. Cascarano, L. De Caro, C. Giacovazzo, G. Polidori, R. Spagna, J. Appl. Cryst. 38 (2005) 381.

[35] G.M. Sheldrick, Acta. Crystallogr., Sect. A. 64 (2008) 112.

[36] *DIRDIF-99*. P. T. Beurskens, G. Beurskens, R. de Gelder, S. Garcia-Granda, R.O. Gould, R. Israel, J. M. M. Smits, Crystallography Laboratory, University of Nijmegen, The Netherlands, 1999.

[37] G. M. Sheldrick, Acta Crystallogr., Sect. C. 71 (2015) 3.

[38] National Committee for Clinical Laboratory Standards (NCCLS), approved standard M7-A3, 3rd edn. NCCLS, Villanova, 1993.

[39] A.W. Bauer, W.M.M. Kirby, J.C. Sherris, M. Turck, Am. J. Clin. Pathol. 45 (1966) 493.

[40] D. Parai, E. Islam, J. Mitra, S.K. Mukherjee, Can. J. Microbiol. 63 (2017) 169.

[41] C.Z. Chen, S.L. Cooper, Biomaterials 23(16) (2002) 3359.

[42] W.J. Geary, Coord. Chem. Rev. 7 (1971) 81.

[43] N.C. Saha, R.J. Butcher, S. Chaudhuri, N. Saha, Polyhedron 22 (2003) 383 (and references therein).

[44] A.B.P. Lever, Inorganic Electronic Spectroscopy, Elsevier, New York, 1984, 507.

[45] P. Bera, N. C. Saha, J. Ind. Chem. Soc. 87 (2010) 919.

[46] A.W. Addison, T.N. Rao, J. Reedijk, J. Rijn, G.C. Verschoor, Dalton Trans. 1 (1984) 1349.

[47] L. Qiu, J. Lin, Y. Xu, Inorg. Chem. Communications 12 (2009) 986 (and references therein)

[48] D.M. Boghaei, F. Behzadian-Asl, Journal of Coordination Chemistry 60 (2007) 347

[49] M. Guerrero, J. Pons, J. Ros, M. Font-Bardia, O. Vallcorba, J. Rius, V. Branchadell, A. Merkoçi, CrystEngComm**,** 2011,**13**, 6457-6470

[50] Z.H. Abd EleWahab, O. A.M. Ali, B.A. Ismail, Journal of Molecular Structure 1144 (2017) 136

[51] (a) D. Majumdar, M.S. Surendra Babu, S. Das, C. Mohapatra, J.K. Biswas, M. Mondal, ChemistrySelect 2 (2017) 4811; (b) D. Majumdar, M.S. Surendra Babu, S. Das, J.K. Biswas, M. Mondal, S. Hazra,. J.Mol. Struct. 1134 (2017) 617.

CAPTIONS TO THE FIGURES

Fig. 1: Structural formulation of the ligand, MP_zOATA.

Fig. 2: Molecular view of complex **I** with atom numbering scheme.

Fig. 3: Molecular view of complex **II** with atom numbering scheme.

Fig. 4: Molecular view of complex **III** with atom numbering scheme.

Fig. 5: Molecular view of complex **IV** with atom numbering scheme.

Fig. 6: Molecular view of complex **V** with atom numbering scheme.

Fig. 7: Fluorescence spectra of complex **IV** [_____ (λ_{emi} = 432nm, λ_{ex}= 336 nm); ____ (λ_{emi} = 503 nm, λ_{ex}= 254 nm)] and complex **V** [_____ (λ_{emi} = 478 nm, λ_{ex} = 251 nm)].

Fig. 8: *In vitro* growth curve of *Enterobacter aerogenes* 10102 against the synthesized complexes: (a) complex **I**, (b) complex **II**, (c) complex **III**, (d) complex **IV** and (e) complex **V**

Fig. 9: *In vitro* growth curve of *Bacillus subtilis* 6633 against the synthesized complexes: (a) complex **I**, (b) complex **II**, (c) complex **III**, (d) complex **IV** and (e) complex **V**

Fig. 10: Membrane damage efficiency of the complexes against (a) *Bacillus subtilis* 6633 and (b) *Proteus vulgaris* OX19.

Fig. S1: View down the *c*-axis of the one-dimensional hydrogen-bonded chain formed in complex **I**, running along the *b*-axis. Hydrogen atoms not involved in hydrogen bonding, and PF_6^- anions are omitted.

Fig. S2: Hydrogen bonding pattern in complex **II.**

Fig. S3: Hydrogen bonding pattern in complex **III.**

Fig. S4: Packing diagram of complex **IV** with N-H...Cl hydrogen bonding interactions.

Fig. S5: Formation of 1D supramolecular chain structure in complex **V** by hydrogen bonding interactions.

Table 1: Crystal data and structure refinement parameters for $C_{24}H_{26}ClF_6N_6NiPS_2$ (**I**), $C_{26}H_{29}Cl_2N_7NiO_8S_2$ (**II**), $C_{24}H_{28}B_2F_8N_6NiOS_2$ (**III**), $Cd(MP_zOATA)Cl_2]_2$ (**IV**) and $[Hg(MP_zOATA)Cl_2]$ (**V**)

Crystal data	Complex **I**	Complex **II**	Complex **III**	Complex **IV**	Complex **V**
Empirical formula	$NiC_{24}H_{26}ClF_6N_6PS_2$	$NiC_{26}H_{29}Cl_2N_7O_8S_2$	$NiC_{24}H_{28}B_2N_6F_8OS_2$	$C_{24}H_{26}Cd_2Cl_4N_6S_2$	$C_{12}H_{13}HgN_3Cl_2S$
Formula weight	701.75	761.29	712.95	829.23	502.80
Temperature (K)	173	295	93	123(2)	123(2)
Radiation [Å]	MoK_α 0.71075	CuK_α 1.54178	MoK_α 0.71075	MoK_α 0.71075	MoK_α 0.71075
Crystal system	Monoclinic	Monoclinic	Monoclinic	Triclinic	Triclinic
space group	C2/c (#15)	$P2_1/n$	$P2_1/n$	P-1	P-1
a (Å) α (°)	19.981(18) 90	8.4990(1) 90	11.019(3) 90	8.6081(5) 93.274(4)	8.4533(4) 68.855(5)
b (Å) β (°)	12.964(10) 109.855(3)	19.1894(3) 93.146(1)	19.796(4) 103.658(6)	9.5951(4) 112.213(6)	9.4004(6)80.265(4)
c (Å) γ (°)	23.805(2) 90	20.2945(3) 90	14.370(4) 90	9.7627(6) 96.384(4)	11.0321(5)68.532(5)
Volume ($Å^3$)	5799.7(9)	3304.86(8)	3045.9(13)	737.56(7)	760.21(7)
Z, Calc. density (Mg/m^3)	8, 1.607	4, 1.530	4, 1.555	1, 1.867	2, 2.197
$\mu(MoK_\alpha)$ [/mm]	10.263	4.016	0.854	1.972	10.600
F(000)	2864	1568	1456	408	472
Crystal size (mm)	0.21 x 0.18 x 0.18	0.5725 x 0.2269 x 0.1056	0.12 x 0.12 x 0.12	0.7708 × 0.3037 × 0.1067	0.41 × 0.35 × 0.12
θ ranges (°)	1.90 to 25.40	4.4to 75.8	0.0 to 25.4	3.11 to 34.94	2.98 to 34.91
Limiting indices	-24<= h <= 24	-6<= h <= 10	-9 <= h <= 13	-13 <= h <= 13	-13 <= h <= 13
	-15 <= k <= 15	-23 <= k <= 24	-23 <= k <= 22	-14 <= k <= 15	-15 <= k <= 15
	-28 <= l <=26	-25 <= l <=23	-17 <= l <= 15	-12 <= l <=15	-13 <= l <= 17
Reflections collected	34924	22823	19060	10310	10475
Unique reflections	5345[R(int)= 0.0520]	6745 [R(int) = 0.025]	5563[R(int)= 0.060]	5965[R(int) = 0.0391	6161[R(int)=0.0351]
Refinement method	Full-matrix least	Full-matrix least	Full-matrix least	Full-matrix least	Full-matrix least
	-squares on F^2	-squares on F^2	-squares on F^2	-squares on F^2	-squares on F^2
Goodness-of-fit on F^2	1.028	1.026	1.058	1.081	1.025
Final R indices [I>2σ (I)]	R1=0.0447	R1 = 0.0484	R1= 3934	R1 = 0.0393	R1= 0.0357
R indices (all data)	R1 = 0.0491	R1 = 0.0569	R1 = 0.0525	R1 = 0.0566	R1 =0.0489
	wR2=0.1214	wR2 = 0.1539	wR2 =0.1258	wR2 = 0.0815	wR2 =0.0587
Largest diff. peak, hole (e. $Å^{-3}$)	-0.53 and 1.04	-0.39and 0.53	-0.43 and -0.51	1.419 and -0.949	1.949 and -1.544

Table 2: Selected bond lengths (Å) and bond angles (º) for $C_{24}H_{26}ClF_6N_6NiPS_2$ (I), $C_{26}H_{29}Cl_2N_7NiO_8S_2$ (II), $C_{24}H_{28}B_2F_8N_6NiOS_2$ (III), $[Cd(MPzOATA)Cl_2]_2$ (IV) and $[Hg(MPzOATA)Cl_2]$ (V)

Complex **I**		Complex **II**		Complex **III**		Complex **IV**		Complex **V**	
Bond lengths (Å)		Bondlengths (Å)		Bond lengths (Å)		Bond lengths (Å)		Bond lengths (Å)	
Ni1–N1	2.044(2)	Ni-N1A	2.042(3)	Ni1 -N9	2.046(3)	Cd-N(1)	2.367(2)	Hg-N(1)	2.413(4)
Ni1 –N2	2.056(3)	Ni -N1B	2.041(2)	Ni1 -N12	2.078(4)	Cd-N(2)	2.383(2)	Hg-N(2)	2.444(3)
Ni1 –N4	2.035(3)	Ni -N2A	2.071(3)	Ni1 -N29	2.045(3)	Cd-Cl(1)	2.496(8)	Hg-S(1)	2.751(10)
Ni1 –N5	2.067(2)	Ni -N2B	2.068(3)	Ni1 -N32	2.068(3)	Cd-Cl(2)	2.526(7)	Hg-Cl(1)	2.415(9)
Ni1 –S1	2.418(10)	Ni -S1A	2.436(9)	Ni1 -S2	2.434(1)	Cd-Cl(2)#1	2.724(7)	Hg-Cl(2)	2.485(9)
Ni1 -S2	2.427(8)	Ni -S1B	2.430(9)	Ni1 -S22	2.415(1)	Cd-S(1)	2.967(7)	N(1)-C(4)	1.350(4)
N1-C2	1.423(4)	N1A-C7A	1.426(4)	N9-C4	1.423(6)	N(2)-C(6)	1.418(3)	C(4)-C(5)	1.455(5)
C1-C2	1.396(5)	C2A-C7A	1.395(5)	C3-C4	1.399(6)	C(6)-C(11)	1.401(3)	C(5)-N(2)	1.271(5)
S1-C1	1.781(3)	S1A -C2A	1.778(3)	S2-C3	1.783(4)	C(11)-S(1)	1.760(3)	N(2)-C(6)	1.416(5)
N1-C8	1.286(4)	N1A-C8A	1.277(4)	N9-C10	1.280(5)	N(1)-C(4)	1.341(3)	C(6)-C(11)	1.400(5)
C8-C9	1.457(5)	C8A-C9A	1.449(5)	C10-C11	1.461(6)	C(4)-C(5)	1.453(4)	C(11)-S(1)	1.770(3)
N2-C9	1.339(4)	N2A-C9A	1.338(4)	C11-N12	1.340(5)	C(5)-N(2)	1.278(3)		
N4-C14	1.413(4)	N1B-C7B	1.423(4)	N29-C24	1.422(5)				
C14-C13	1.388(4)	C2B-C7B	1.390(4)	C24-C23	1.405(5)				
S2-C13	1.787(3)	S1B-C2B	1.778(4)	S22-C23	1.782(4)				
N4-C20	1.302(4)	N1B-C8B	1.281(4)	N29-C30	1.292(5)				
C20-C21	1.428(5)	C8B-C9B	1.453(4)	C30-C31	1.440(5)				
C21-N5	1.333(4)	N2B-C9B	1.340(4)	C31-N32	1.358(5)				
Bond angles (°)		Bond angles (°)		Bond angles (°)		Bond angles (°)		Bond angles (°)	
N1-Ni1-N2	79.17(10)	N1A-Ni-N1B	177.25(10)	N9-Ni1-N12	78.92(12)	S(1)-Cd-N(1)	109.78(6)	N(1)-Hg-N(2)	67.59(11)
N1-Ni1-N4	176.17(11)	N1A-Ni-N2A	78.99(10)	N9-Ni1-N29	176.93(11)	N(1)-Cd-Cl(1)	156.60(7)	S(1)-Hg-N(2)	69.77(8)
N4-Ni1-N5	79.42(10)	N1A-Ni-N2B	97.93(10)	N9-Ni1-N32	97.55(12)	N(2)-Cd-Cl(1)	102.14(6)	S(1)-Hg-N(1)	123.41(7)
N2-Ni1-N4	98.89(11)	N1B-Ni-N2A	101.17(10)	N12-Ni1-N29	100.65(12)	N(1)-Cd-Cl(2)	95.84(6)	Cl(1)-Hg-Cl(2)	115.11(3)
N1-Ni1-N5	103.74(10)	N1B-Ni-N2B	79.33(10)	N12-Ni1-N32	92.87(12)	N(2)-Cd-Cl(2	136.96(6)	Cl(1)-Hg-S(1)	119.40(3)
N2-Ni1-N5	88.20(11)	N2A-Ni-N2B	92.89(10)	N29-Ni1-N32	79.41(12)	Cl(1)-Cd-Cl(2	104.41(3)	Cl(1)-Hg-N(1)	108.24(8)
S1-Ni1-S2	91.31(3)	S1A-Ni-S1B	85.03(3)	S2-Ni1-S22	84.93(4)	N(1)-Cd-Cl(2)#1	80.72(6)	Cl(1)-Hg-N(2)	108.33(7)
S1-Ni1-N1	82.77(8)	S1A-Ni-N1A	82.75(7)	S2-Ni1-N9	83.14	N(2)-Cd-Cl(2)#1	123.84(5)	Cl(2)-Hg-S(1)	86.98(3)
S1-Ni1-N2	160.83(7)	S1A-Ni-N1B	97.30(7)	S2-Ni1-N12	161.55(9)	Cl(1)-Cd-Cl(2)#1	87.30(2)	Cl(2)-Hg-N(1)	99.51(8)
S1-Ni1-N4	99.50(9)	S1A-Ni-N2A	161.12(7)	S2-Ni1-N29	97.52	Cl(2)-Cd-Cl(2)#1	90.80(2)	Cl(2)-Hg-N(2)	136.51(7)
S1-Ni1-N5	89.88(9)	S1A-Ni-N2B	94.34(8)	S2-Ni1-N32	93.61(10)	N(2)-Cd-S(1)	63.68(5)		
S2-Ni1-N5	162.46(8)	S1B-Ni-N2A	93.27(7)	S22-Ni1-N12	93.95(9)	Cl(1)-Cd-S(1)	83.44(2)		
S2-Ni1-N1	93.77(6)	S1B-Ni-N2B	162.23(8)	S22-Ni1-N9	99.67	Cl(2)-Cd-S(1)	86.41(2)		
S2-Ni1-N4	83.12(7)	S1B-Ni-N1A	99.60(7)	S22-Ni1-N29	83.40	Cl(2)#1-Cd-S(1)	169.34(2)		
S2-Ni1-N2	96.23(7)	S1B-Ni-N1B	83.14(7)	S22-Ni1-N32	162.41(8)	N(1)-Cd-N(2)	69.11(8)		

Table 3: MIC values (µg/mL) of the synthesized complexes against the selected bacterial strains

Organisms	Complex I	Complex II	Complex III	Complex IV	Complex V	Amoxicillin
Escherichia coli K12	1575	1450	1550	175	20	7
Salmonella enterica ser. typhi SRC	1550	1000	1550	45	55	31
Proteus vulgaris OX19	1300	1450	975	35	5	129
Bacillus subtilis 6633	1225	1050	750	40	25	28
Staphylococcus aureus	1275	1625	1225	25	20	85
Enterobacter aerogenes 10102	1300	1425	1400	175	35	280

Table 4: Growth inhibition zone diameter of MIC (mm) of synthesized complexes against the selected bacterial strains

Organism	Complex I	Complex II	Complex III	Complex IV	Complex V	Amoxicillin
Escherichia coli K12	4.3±0.2	3.2±0.3	3.7±0.5	4.2 ±0.4	2.5±0.2	12.3±0.4
Salmonella enteric ser. typhi SRC	1.9±0.1	6.8±0.2	2.1±0.3	2.5±0.1	3.1±0.2	9.4±0.2
Proteus vulgaris OX19	2.1±0.1	2.2±0.1	2.5±0.2	3.8±0.2	6.9±0.5	7.6±0.5
Bacillus subtilis 6633	6.8±0.3	3.8±0.3	6.5±0.4	5.5±0.3	7.6±0.5	8.5±0.1
Staphyloccus aureus	2.1±0.1	2.3±0.3	1.8±0.2	3.5±0.1	8.5±0.5	7.2±0.6
Enterobacter aerogenes 10102	6.2±0.4	2.5±0.4	4.1±0.2	5.5±0.3	4.1±0.2	8.4±0.5

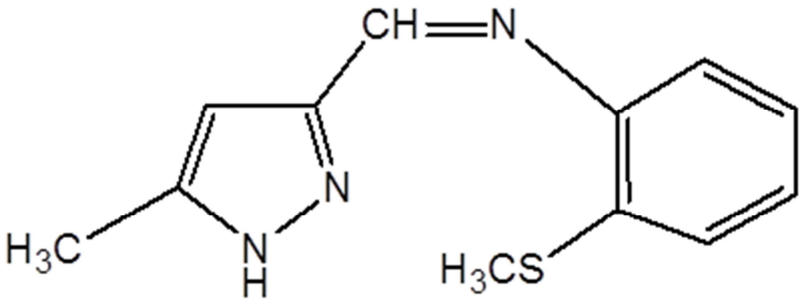

Figure 1

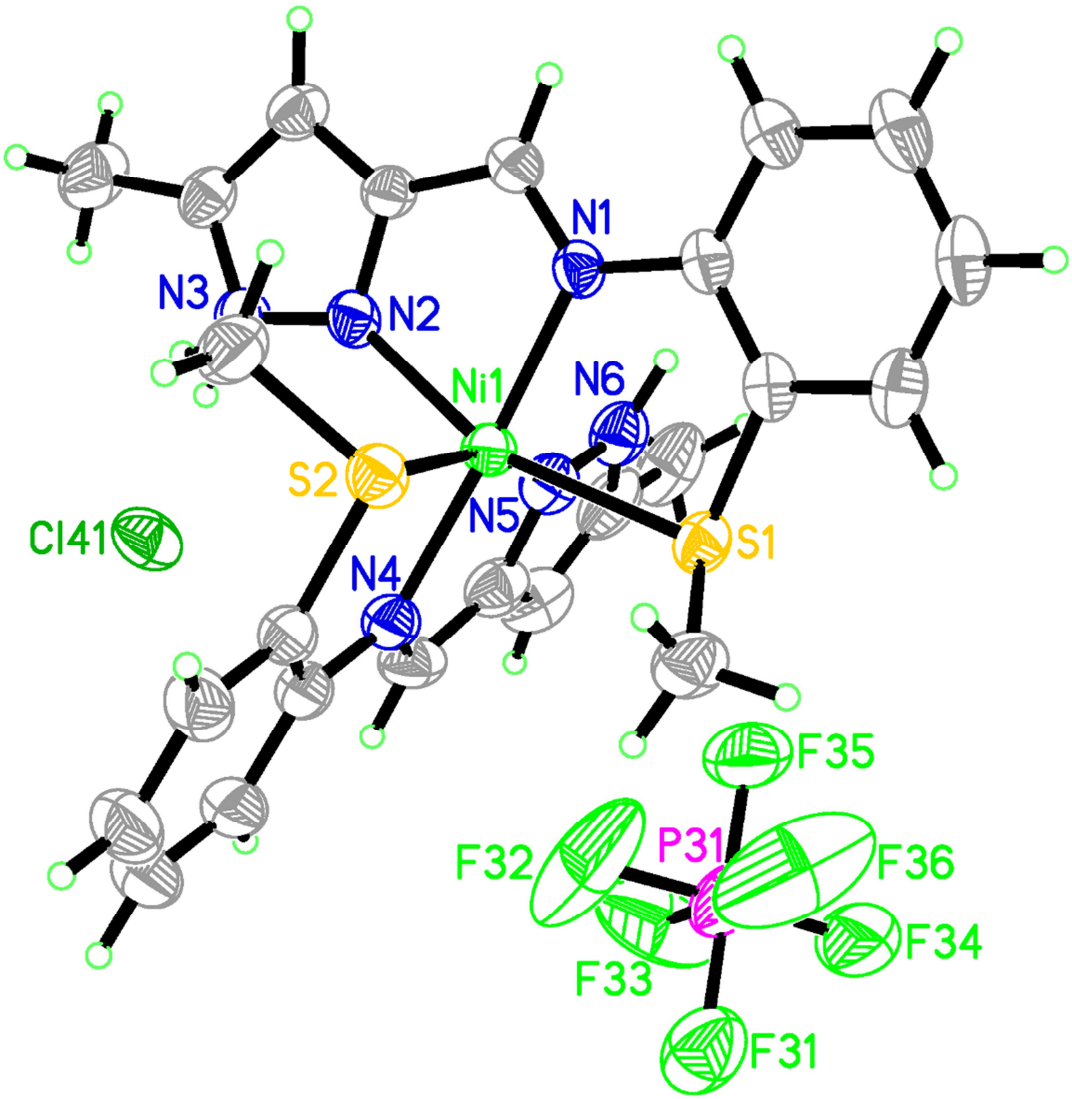

Figure 2

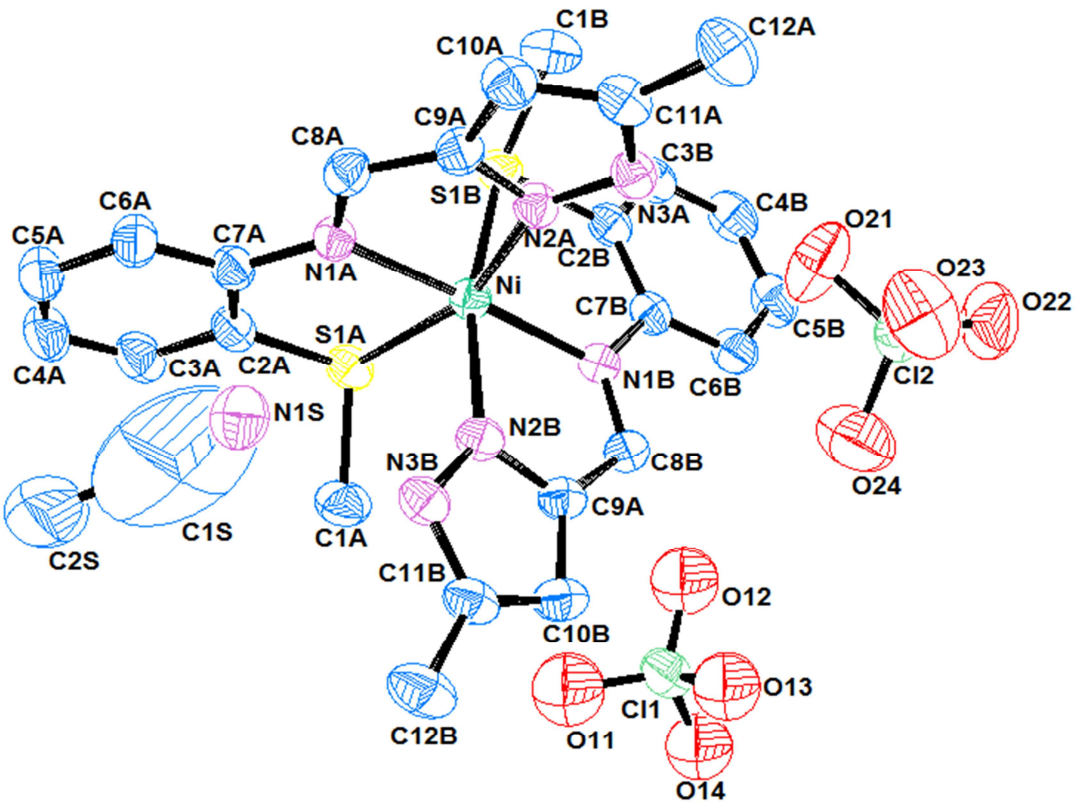

Figure 3

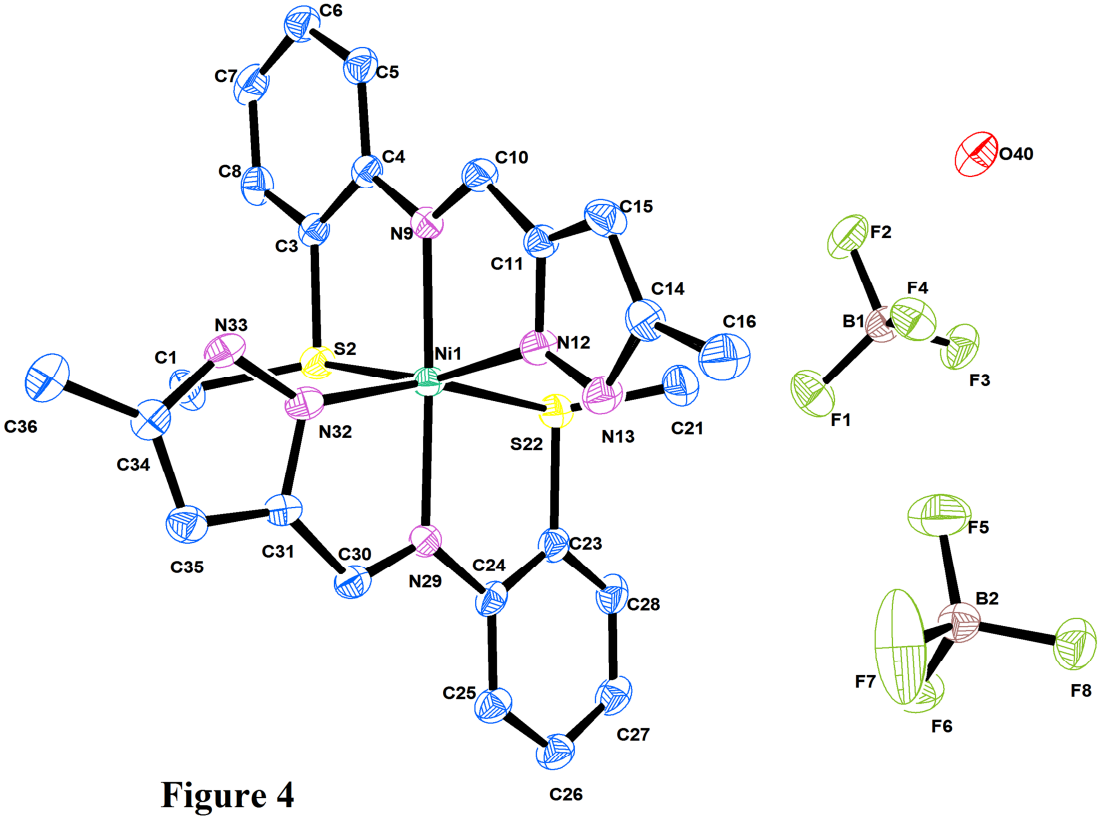

Figure 4

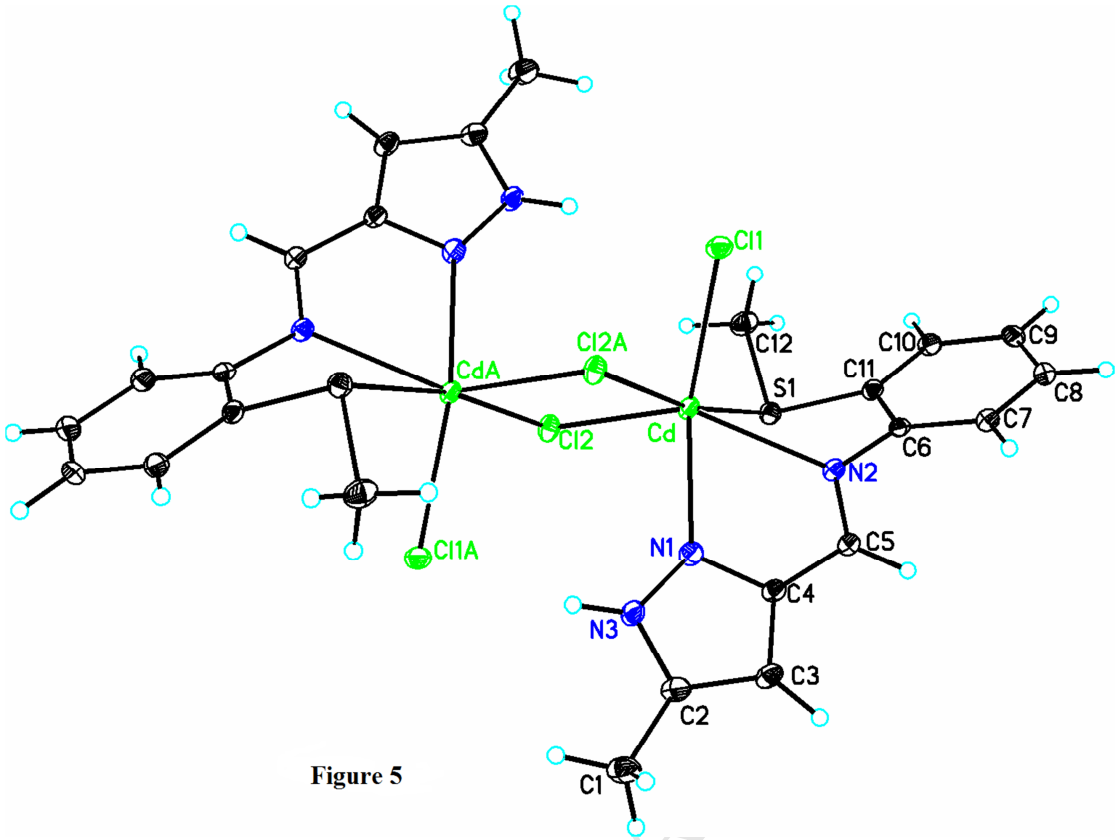

Figure 5

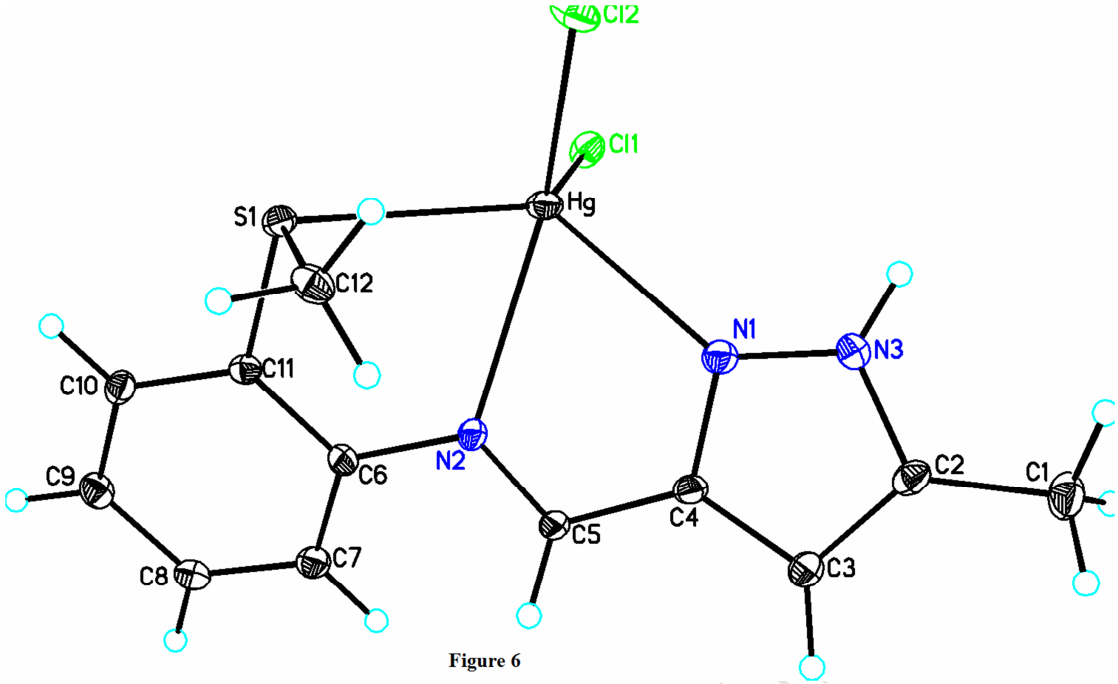

Figure 6

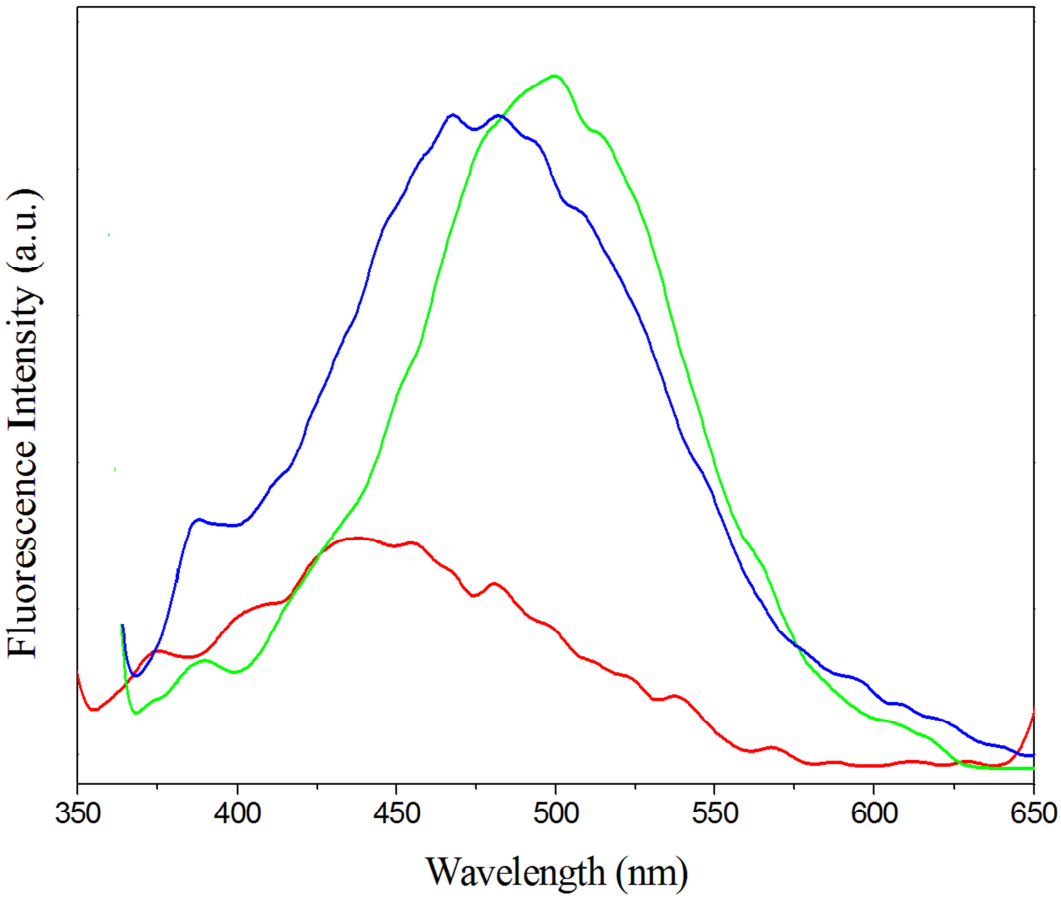

Figure 7

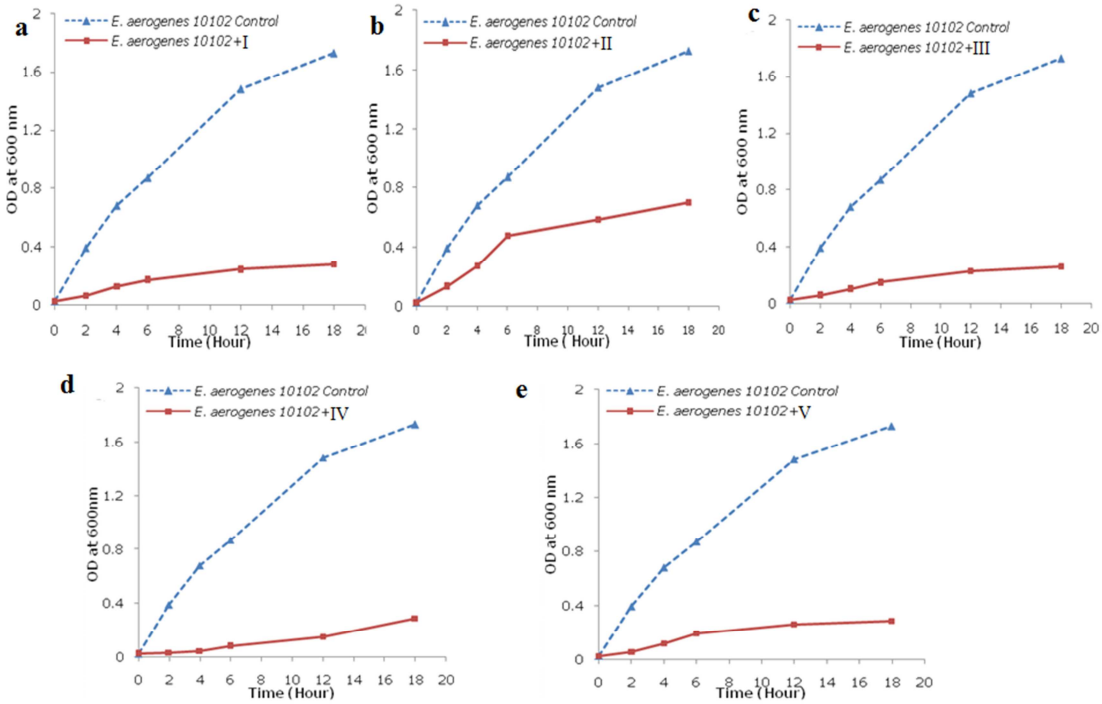

Figure 8

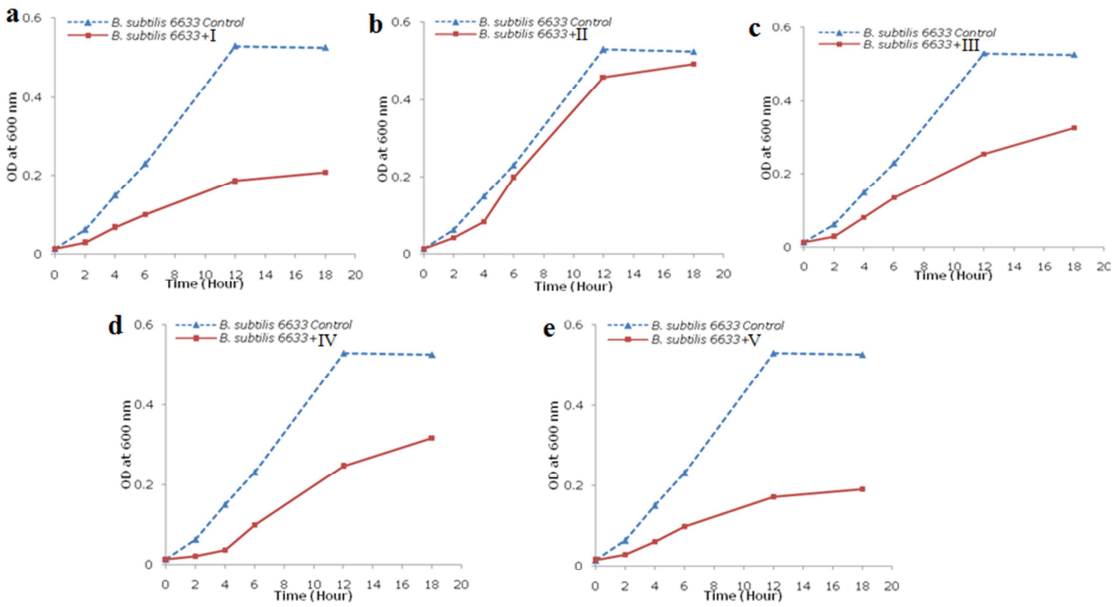

Figure 9

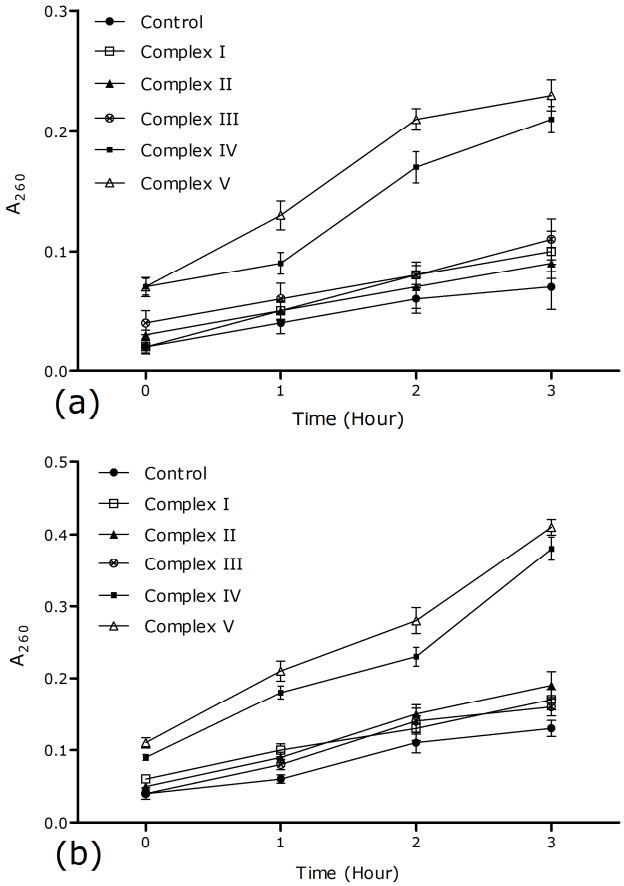

Figure 10

Highlights (for review)

Syntheses, physico-chemical and spectroscopic characterizations of five new Ni(II), Cd(II) & Hg(II) complexes of a pyrazole containing Schiff-base ligand have been reported.

X-ray crystallographic studies on all the reported complex species have authenticated the structures of the complexes as envisaged from spectroscopy.

Photoluminescence property of the complexes has been studies; Cd(II) and Hg(II) complexes have been shown to be fluorescence active.

Antimicrobial activities of the complexes against some Gram positive and Gram negative bacteria have been reported, and the complexes have been found to be the potential antimicrobial agents in broad spectrum against the both.